Statistical properties of stochastic functionals under general resetting

Vicenç Méndez * and Rosa Flaquer-Galmés *

Grup de Física Estadística, Departament de Física, Facultat de Ciències, Universitat Autònoma de Barcelona, 08193 Barcelona, Spain

(Received 3 July 2025; revised 26 August 2025; accepted 22 September 2025; published 14 October 2025)

We derive the characteristic function of stochastic functionals of a random walk whose position is reset to the origin at random times drawn from a general probability distribution. We analyze the long-time behavior and obtain the temporal scaling of the first two moments of any stochastic functional of the random walk when the resetting time distribution exhibits a power-law tail. When the resetting times probability density function has finite moments, the probability density of any functional converges to a delta function centered at its mean, indicating an ergodic phase. We explicitly examine the case of the half-occupation time and derive the ergodicity breaking parameter, the first two moments, and the limiting distribution when the resetting time distribution follows a power-law tail, for both Brownian and subdiffusive random walks. We characterize the three different shapes of the limiting distribution as a function of the exponent of the resetting distribution. Our theoretical findings are supported by Monte Carlo simulations, which show excellent agreement with the analytical results.

DOI: 10.1103/pcm7-bw2y

I. INTRODUCTION

In recent years, stochastic resetting has emerged as a powerful concept in the study of random processes, attracting growing attention across various disciplines. This mechanism, which intermittently interrupts the evolution of a stochastic process by returning it to a predefined state, has been shown to significantly alter fundamental properties of the underlying random walk. Originally proposed in the context of Brownian motion [1,2] stochastic resetting has since been extended to a wide range of processes, including Lévy flights [3-5], run-and-tumble dynamics [6], and subdiffusive motion [7]. Notably, resetting can lead to the formation of a nonequilibrium stationary state and optimize search strategies by minimizing the mean first passage time under certain conditions. This effect is due to the fact that stochastic resetting forces the walker to revisit a point or a region [8]. A similar effect is observed when the walker moves in a heterogeneous media in which the diffusion coefficient depends on space as power law [9] or when the walker is under the effect of a force field [10,11], the system reaches a steady state and the mean first passage is finite. Most of the studies deal with a Poissonian resetting process, i.e., when the reset times are distributed according to an exponential distribution. Only a few studies deal with reset times distributed according to general distributions. If this distribution decays as a power-law, then the existence of a steady state and a finite first passage time depend on the characteristic exponent of the distribution and the properties of the underlying random walk [12–16].

On the other hand, in the last decades stochastic functionals have received much attention. The prototypical example of stochastic functional is the Brownian functional, defined as the time-integral over the trajectory of a walker when it is

*Contact author: vicenc.mendez@uab.cat

Brownian. In 1949 [17] Kac realized that the statistical properties of one-dimensional Brownian functionals can be studied by celebrated Feynman-Kac formula. Since then Brownian functionals have found numerous applications in diverse fields ranging from probability theory [18,19] and finance [20] to disordered systems and mesoscopic physics [21] and computer science [22]. More recently, the case of subdiffusive walkers has been considered as well [23,24]. Among the most widely studied functionals are the occupation time in an interval and the half-occupation time, which have diverse applications in physics, mathematics, and related fields [25].

Another problem involving resetting consists of studying the statistical properties of stochastic functionals of a random walker when its position is forced to start anew at random times. Most existing studies regarding stochastic functionals under resetting consider it as Poissonian process [26,27], and less attention is paid when the resetting times are distributed according to general probability density functions. However, we have recently studied the statistical properties of the occupation time in an interval for a Brownian particle under reset times sampled from a power-law probability density function (PDF) [28]. Despite this progress, a comprehensive theory describing the behavior of general stochastic functionals under arbitrary resetting schemes is still lacking.

In this work, we explore how the statistical properties of stochastic functionals are affected when the position of the underlying random walk is reset to the origin after random times sampled from a general PDF. Since the resetting mechanism is a renewal process, we are able to find an equation that relates the characteristic function of the functional under resetting in terms of two expressions: the resetting times PDF and the characteristic function of the functional without resetting. We find that when the moments of the resetting PDF are finite, the PDF of the functional converges to a delta function centered at the mean value in the long-time limit. This is the ergodic case.

On the other hand, when the resetting times PDF has diverging moments, the characteristic function must be computed on a case-by-case basis, specifying each functional individually. We further explore the temporal behavior of the first two moments of the functional, which is also useful to study the ergodic properties. We particularize our general results to the half occupation time and obtain its limiting PDF when the resetting times PDF has a power-law tail. More specifically, we obtain the limiting PDF for both normal and subdiffusive underlying random walks.

The paper is structured as follows: In Sec. II we introduce the definition of stochastic functional and its characteristic function (or moment-generating function). In Sec. III we derive the characteristic function of a functional under general resetting, obtain the expression for the first two moments, and illustrate how to analyze the ergodic properties. In Sec. IV we prove general results for any stochastic functional. In particular, we show that any stochastic functional becomes ergodic, i.e., deterministic in the long-time limit, when the resetting PDF has finite moments. Likewise, we derive the long-time scaling temporal dependence for the first two moments of any functional when the resetting PDF decays as a power law. In Sec. V we apply our results to the particular case of the half occupation time. We conclude in Sec. VI

II. STOCHASTIC FUNCTIONALS

A stochastic functional is defined as the integral up to the measurement time t of a positive function $U[x(\tau)]$ of the trajectory $\{x(\tau); 0 \leqslant \tau \leqslant t, x(0) = x_0\}$ of a random walker. The stochastic functional is then given by

$$Z(t|x_0) = \int_0^t U[x(\tau)]d\tau, \tag{1}$$

where U(x) is some prescribed arbitrary function. For example, if $U(x) = \theta(x)$ ($\theta(x)$ is the Heaviside function) then $Z(t|x_0)$ is the half occupation time, this is, the time spent by the random walker in the positive half-space. Since x(t) is a stochastic process, $Z(t|x_0)$ is also a stochastic process. For each realization of the walker's path, the quantity $Z(t|x_0)$ has a different value and one is interested in the PDF of $Z(t|x_0)$, say $P(Z,t|x_0)$. $P(Z,t|x_0)$ is then the probability that the functional takes the value Z at time t given that the walker was initially at $x = x_0$. Let $Q(p,t|x_0)$ be the characteristic function (or moment-generating function) of $Z(t|x_0)$, which can be expressed as the Laplace transform with respect to Z, this is,

$$Q(p,t|x_0) = \mathcal{L}_{Z \to p}[P(Z,t|x_0)] = \int_0^\infty e^{-pZ} P(Z,t|x_0) dZ$$
$$= \langle e^{-pZ(t|x_0)} \rangle = \langle e^{-p\int_0^t U[x(\tau)]d\tau} \rangle, \tag{2}$$

which satisfies a backward master equation known as the Feynman-Kac equation [17,18]. Expanding the exponential in (2) as a power series, we find

$$Q(p,t|x_0) = \left\langle \sum_{n=0}^{\infty} \frac{(-p)^n}{n!} Z(t|x_0)^n \right\rangle = \sum_{n=0}^{\infty} \frac{(-p)^n}{n!} \langle Z(t|x_0)^n \rangle.$$
(3)

Introducing another Laplace transform conjugate to time as

$$\tilde{Q}(p, s|x_0) = \mathcal{L}_{t \to s}[Q(p, t|x_0)] = \int_0^\infty dt \ e^{-st} Q(p, t|x_0),$$
 (4)

the moments of $Z(t|x_0)$ can be obtained from the derivatives of $\tilde{Q}(p, s|x_0)$ in a systematic manner. To do this, we first define the Laplace transform of the moments

$$\langle \tilde{Z}(s|x_0)^n \rangle \equiv \mathcal{L}_{t \to s} [\langle Z(t|x_0)^n \rangle]$$

$$= \int_0^\infty dt e^{-st} \int_0^\infty Z(t)^n P(Z, t|x_0) dZ. \tag{5}$$

Making use of Eq. (2), it is straightforward to show that the moments are represented in terms of the generating function in the following way:

$$\langle \tilde{Z}(s|x_0)^n \rangle = (-1)^n \frac{\partial^n \tilde{Q}(p, s|x_0)}{\partial p^n} \bigg|_{p=0}.$$
 (6)

This equation will be used later to compute the moments of the functional once the characteristic function is known.

III. CHARACTERISTIC FUNCTION UNDER RESETTING

The goal is to compute the characteristic function of a stochastic functional $Z(t|x_0)_r$ when the underlying random walk is subjected to resetting the position to $x = x_0$. The random walk process under resetting is as follows. The walker starts moving at $x = x_0$, a positive resetting time τ_1 is drawn from the PDF $\varphi(\tau)$ and the walker performs a free random walk in the interval of time $(0, \tau_1)$, finally reaching some random position. Then the walker's position is reset instantaneously to $x = x_0$, and the process is then renewed, namely, a second resetting time τ_2 is drawn also from $\varphi(\tau)$, etc. When this process is continued we get the sequence of independent identically distributed random variables, $\{\tau_1, \tau_2, ...\}$, i.e., the waiting times between resetting events, which are needed to construct the path of the particle. Consider now that there are N resets in the time interval (0, t). Thus

$$t = \sum_{l=1}^{N} \tau_l + B,\tag{7}$$

where B is the time since the last reset (the backward recurrence time). In consequence, the integral in Eq. (1) can be expressed as the sum of the contributions over the interresetting periods

$$Z(t|x_{0})_{r} = \int_{0}^{\tau_{1}} U[x(t')]dt' + \int_{\tau_{1}}^{\tau_{1}+\tau_{2}} U[x(t')]dt' + \cdots$$

$$+ \int_{\tau_{1}+\dots+\tau_{N-1}}^{\tau_{1}+\dots+\tau_{N-1}+\tau_{N}} U[x(t')]dt' + \int_{\tau_{1}+\dots+\tau_{N}}^{t} U[x(t')]dt'$$

$$= \sum_{l=1}^{N} \int_{\delta_{l}}^{\tau_{l}+\delta_{l}} U[x(t')]dt' + \int_{\delta_{N+1}}^{t} U[x(t')]dt', \qquad (8)$$

where $\delta_l = \sum_{j=0}^{l-1} \tau_j$ and $\tau_0 = 0$. Since $\varphi(\tau)$ is the PDF of waiting times between two consecutive resets,the probability of no reset until time τ is

$$\varphi^*(\tau) = 1 - \int_0^{\tau} \varphi(\tau') d\tau' = \int_{\tau}^{\infty} \varphi(\tau') d\tau'.$$

Because of the additive form of $Z(t|x_0)_r$, it is clear that its characteristic function $Q(p, t|x_0)_r$ can be decomposed, when conditioned on these N resettings, into a product of generating functions involving only free random walk between resettings. To write the full $Q(p, t|x_0)_r$, we then have to sum over all possible number of resets and reset times. Then, the characteristic function $Q(p, t|x_0)_r$ of the functional $Z(t|x_0)_r$, can be written in the form of a renewal equation [26]

$$Q(p, t|x_0)_r = \sum_{N=0}^{\infty} \int_0^t F(p, \tau_1) d\tau_1 \int_0^t F(p, \tau_2) d\tau_2$$

$$\cdots \int_0^t F(p, \tau_N) d\tau_N$$

$$\times \int_0^t F^*(p, B) \delta\left(t - \sum_{l=1}^N \tau_l - B\right) dB, \quad (9)$$

where $Q(p, t|x_0)_0$ is the characteristic function of Z when the underlying random walk is free of resetting. We have also defined $F(p, \tau_l) = \varphi(\tau_l)Q(p, \tau_l|x_0)_0$ for l=1,...,N and $F^*(p,B) = \varphi^*(B)Q(p,B|x_0)_0$. The product of the N integrals of $F(p,\tau_l)$ are the contributions to $Q(p,t|x_0)_r$ from the N resets in (0,t) and the integral of $F^*(p,\tau_l)$ is the contribution when no reset occurs during the backward time B. It is interesting to emphasize that B does not have the same PDF as the waiting times between resets $\{\tau_1,...,\tau_N\}$, except when the resetting renewal process is Markovian, i.e., when the resets are following a Poisson process with exponentially distributed waiting times between resets (see, e.g., Ref. [25,29] and [30] for discrete reset times)

A standard method for solving such an equation is to use the Laplace transform with respect to the variable t. For example, if there is only one reset in (0, t), the contribution to $Q(p, t|x_0)_r$ is

$$Q_{N=1}(p, t | x_0)_r = \int_0^t d\tau_1 F(p, \tau_1) \int_0^t dB F^*(p, B) \times \delta(t - \tau_1 - B).$$

whose Laplace transform is $\tilde{Q}_{N=1}(p,s|x_0)_r = \mathcal{L}_{t\to s}$ $[\tilde{Q}_{N=1}(p,t|x_0)_r] = F(p,s)F^*(p,s)$, once the convolution theorem is used. Analogously, if there are two resets in (0,t), the contribution to $Q(p,t|x_0)_r$ is $\tilde{Q}_{N=2}(p,s|x_0)_r = F(p,s)^2F^*(p,s)$ and so on. Then summing the contributions from all the possibles resets in (0,t) we have that (9) turns into

$$\tilde{Q}(p, s|x_0)_r = \sum_{N=0}^{\infty} F(p, s)^N F^*(p, s) = \frac{F^*(p, s)}{1 - F(p, s)}
= \frac{\mathcal{L}_{t \to s} [\varphi^*(t) Q(p, t|x_0)_0]}{1 - \mathcal{L}_{t \to s} [\varphi(t) Q(p, t|x_0)_0]},$$
(10)

in the Laplace space. This equation allows to find the characteristic function of a functional of a random walk under resetting in terms of the characteristic function of the functional of a random walk without resetting. Note that in the absence of resetting $\varphi \to 0$ and $\varphi^* \to 1$, so that $\tilde{Q}(p, s|x_0)_r = \tilde{Q}(p, s|x_0)_0$.

When the resetting mechanism is a Poisson process, the times between resetting events are exponentially distributed with the constant rate r. Then, considering the particular case $\varphi(t) = re^{-rt}$, Eq. (10) turns out to be

$$\tilde{Q}(p, s|x_0)_r = \frac{\tilde{Q}(p, s + r|x_0)_0}{1 - r\tilde{Q}(p, s + r|x_0)_0}$$
(11)

which is a result derived previously in Refs. [26,27].

A. Moments

Next, we want to relate the moments of the functional in the presence of resetting with the moments of the functional without resetting. To do this, we start with Eq. (10). Taking the first derivative of Eq. (10) with respect to p we find from Eq. (6)

$$\langle \tilde{Z}(s|x_0) \rangle_r = -\frac{\partial \tilde{Q}(p, s|x_0)_r}{\partial p} \bigg|_{p=0} = -\frac{\partial}{\partial p} \left(\frac{F^*(p, s)}{1 - F(p, s)} \right)_{p=0}$$

$$= -\frac{1}{1 - F(0, s)} \frac{\partial F^*(p, s)}{\partial p} \bigg|_{p=0}$$
(12)

$$= -\frac{1}{1 - F(0, s)} \frac{\partial F(p, s)}{\partial p} \Big|_{p=0}$$

$$-\frac{F^*(0, s)}{[1 - F(0, s)]^2} \frac{\partial F(p, s)}{\partial p} \Big|_{p=0},$$
(13)

where $F(0, \tau) = \varphi(\tau)$ and $F^*(0, \tau) = \varphi^*(\tau)$. Hence,

$$\langle \tilde{Z}(s|x_0) \rangle_r = \frac{\mathcal{L}_{t \to s} [\varphi^*(t) \langle Z(t|x_0) \rangle_0]}{1 - \varphi(s)} + \frac{\mathcal{L}_{t \to s} [\varphi(t) \langle Z(t|x_0) \rangle_0]}{s[1 - \varphi(s)]}.$$
(14)

Analogously, taking the second derivative of Eq. (10) with respect to p, we straightforwardly find

$$\langle \tilde{Z}(s|x_0)^2 \rangle_r = \frac{2\mathcal{L}_{t\to s}[\varphi(t)\langle Z(t|x_0)\rangle_0]}{1-\varphi(s)} \langle \tilde{Z}(s|x_0)\rangle_r + \frac{1}{1-\varphi(s)} \left\{ \mathcal{L}_{t\to s}[\varphi^*(t)\langle Z(t|x_0)^2\rangle_0] + \frac{1}{s} \mathcal{L}_{t\to s}[\varphi(t)\langle Z(t|x_0)^2\rangle_0] \right\}. \tag{15}$$

Following the steps above, we can obtain the corresponding expressions for higher-order moments.

B. Ergodic properties

In recent years there was much interest in studying the ergodic properties of certain observables defined as functions anomalous diffusion paths [31–35]. The ergodicity breaking parameter is a measure for the heterogeneity among different trajectories of one ensemble and provides useful statistical information. Let us consider a stochastic trajectory $\{x(\tau); 0 \le \tau \le t, x(0) = x_0\}$, i.e., observed from $\tau = 0$ up to time $\tau = t$. Consider an observable $\mathcal{O}[x(\tau)]$, a function of the trajectory $x(\tau)$. Since $x(\tau)$ is stochastic in nature, the observable $\mathcal{O}[x(\tau)]$ will also fluctuate between the realizations. An observable of the random walk is said to be ergodic if the ensemble average equals the time average $\langle \mathcal{O} \rangle = \overline{\mathcal{O}}$ in the long-time limit. This means that if $\mathcal{O}[x(\tau)]$ is ergodic then its time average $\overline{\mathcal{O}}$ is not a random variable. As a consequence, the limiting PDF (the PDF in the long-time limit) of $\overline{\mathcal{O}}$ is a

delta function centered on its ensemble average, that is,

$$P(\overline{\mathcal{O}}, t \to \infty) = \delta(\overline{\mathcal{O}} - \langle \overline{\mathcal{O}} \rangle). \tag{16}$$

At this point, let us define the density P(x, t) as the probability of finding the walker at the point x at time t, i.e., it is the propagator. If the observable is integrable with respect to the density P(x, t), then the ensemble average is

$$\langle \mathcal{O}[x(t)] \rangle = \int_{-\infty}^{\infty} \mathcal{O}[x] P(x, t) dx,$$
 (17)

while the time average of $\mathcal{O}[x(t)]$ is defined as

$$\overline{\mathcal{O}[x(t)]} = \frac{1}{t} \int_0^t \mathcal{O}[x(\tau)] d\tau. \tag{18}$$

For nonergodic observables, since $\overline{\mathcal{O}}$ is random, its variance $\operatorname{Var}(\overline{\mathcal{O}})$ is nonzero in the long-time limit. Otherwise, for an ergodic observable $\lim_{t\to\infty} \operatorname{Var}(\overline{\mathcal{O}}) = 0$. Keeping this in mind, one can define the ergodicity breaking parameter EB in the following way:

$$EB = \lim_{t \to \infty} \frac{Var(\overline{\mathcal{O}})}{\langle \overline{\mathcal{O}} \rangle^2} = \lim_{t \to \infty} \frac{\langle \overline{\mathcal{O}}^2 \rangle - \langle \overline{\mathcal{O}} \rangle^2}{\langle \overline{\mathcal{O}} \rangle^2}.$$
 (19)

For ergodic observables, one should have EB = 0.

In the examples below we consider the observable $\mathcal{O}[x(t)] = U[x(t)]$ so that the time average of the observable is from Eq. (18)

$$\overline{\mathcal{O}[x(t)]} = \frac{1}{t} \int_0^t U[x(\tau)] d\tau = \frac{Z(t)}{t}.$$
 (20)

and so

$$\langle \overline{\mathcal{O}} \rangle = \frac{\langle Z(t) \rangle}{t}, \quad \langle \overline{\mathcal{O}}^2 \rangle = \frac{\langle Z(t)^2 \rangle}{t^2}.$$
 (21)

Finally, from Eq. (19) the ergodicity breaking parameter can be expressed in terms of the two first moments of the functional

$$EB = \frac{\langle Z(t)^2 \rangle}{\langle Z(t) \rangle^2} - 1 \tag{22}$$

as $t \to \infty$. Another quantity of interest that characterizes ergodicity is the PDF of the time averaged observable $\overline{\mathcal{O}[x(t)]}$ around its mean for long-times, so we define the dimensionless random variable

$$\eta = \lim_{t \to \infty} \frac{\overline{\mathcal{O}}}{\langle \overline{\mathcal{O}} \rangle} \tag{23}$$

and from Eqs. (20) and (21), the relative time averaged observable U[x(t)] is defined by

$$\eta = \lim_{t \to \infty} \frac{Z(t)}{\langle Z(t) \rangle}.$$
 (24)

Once P(Z, t|0) is known, the PDF of η follows from

$$P(\eta) = P(Z = \eta \langle Z(t) \rangle, t) \langle Z(t) \rangle. \tag{25}$$

It is interesting to note that the variance of η is nothing but the ergodicity breaking parameter:

$$\operatorname{Var}(\eta) = \langle \eta^2 \rangle - \langle \eta \rangle^2 = \langle \eta^2 \rangle - 1 = \frac{\langle Z(t)^2 \rangle}{\langle Z(t) \rangle^2} - 1 = \operatorname{EB}.$$

Therefore, for ergodic observables (EB = 0) one has that the limiting PDF of the time averaged observable is $P(\eta) = \delta(\eta - 1)$.

IV. GENERAL RESULTS

In this section we derive some results for any stochastic functional of a random walk.

A. Limiting PDF

We consider a resetting time PDF with finite moments. In this case, the Laplace transform of the PDF is, in the long-time limit $(s \to 0)$, $\varphi(s) \simeq 1 - \langle t \rangle_R s + \cdots$ where $\langle t \rangle_R$ is the mean resetting time. Expressing the term $\exp(-st)$ as a power series we can write

$$\mathcal{L}_{t\to s}[\varphi(t)\langle Z(t|x_0)\rangle_0] = \sum_{n=0}^{\infty} \frac{(-s)^n}{n!} \int_0^{\infty} t^n \varphi(t)\langle Z(t|x_0)\rangle_0 dt.$$
(26)

Most functionals fulfill $\langle Z(t|x_0)\rangle_0 \sim t^\mu$ in the long-time limit, where μ is a positive real number. The specific value of μ depends on the specific dependence of $U[\cdot]$ on $x(\tau)$ and on the underlying random walk. Then,

$$\int_0^\infty t^n \varphi(t) \langle Z(t|x_0) \rangle_0 dt \sim \int_0^\infty t^{n+\mu} \varphi(t) dt = \langle t^{n+\mu} \rangle_R < \infty,$$
(27)

where $\langle t^{n+\mu} \rangle_R$ is the moment of order $n + \mu$ of the ressetting time PDF which is finite for any n. In consequence we can approximate the expansion (26) as

$$\mathcal{L}_{t\to s}[\varphi(t)\langle Z(t|x_0)\rangle_0] = \int_0^\infty \varphi(t)\langle Z(t|x_0)\rangle_0 dt + O(s).$$

Analogously,

$$\mathcal{L}_{t\to s}[\varphi^*(t)\langle Z(t|x_0)\rangle_0] = \int_0^\infty \varphi^*(t)\langle Z(t|x_0)\rangle_0 dt + O(s).$$

Then, taking the limit $s \to 0$ to Eq. (14) we find

$$\langle \tilde{Z}(s|x_0) \rangle_r \simeq \frac{1}{\langle t \rangle_R s^2} \int_0^\infty \varphi(\tau) \langle Z(\tau|x_0) \rangle_0 d\tau,$$

which after Laplace inversion yields

$$\langle Z(t|x_0)\rangle_r \simeq \frac{t}{\langle t\rangle_R} \int_0^\infty \varphi(\tau) \langle Z(\tau|x_0)\rangle_0 d\tau.$$
 (28)

Proceeding analogously with Eq. (15) and considering a power dependence of $\langle Z(t|x_0)^2 \rangle_0$ on time, we obtain

$$\langle Z(t|x_0)^2 \rangle_r \simeq \frac{t^2}{\langle t \rangle_R^2} \left[\int_0^\infty \varphi(\tau) \langle Z(\tau|x_0) \rangle_0 d\tau \right]^2.$$
 (29)

In consequence, by virtue of Eq. (22), we obtain EB = 0 and the observable $\mathcal{O}[x(t)] = U[x(t)]$ is ergodic, which means that in the long-time limit

$$P(Z, t|x_0)_r = \delta(Z - \langle Z(t|x_0)\rangle_r), \tag{30}$$

where $\langle Z(t|x_0)\rangle_r$ is given by Eq. (28). Changing the PDF in Eq. (30) to the variable $\eta = Z/\langle Z(t|x_0)\rangle_r$ one has

$$P(\eta|x_0)_r = \delta(\eta - 1). \tag{31}$$

It is worth mentioning that we have been able to find the limiting PDF given by Eq. (31) from the two first moments of Z only due to the ergodicity of the observable U[x(t)] when the resetting PDF has finite moments. However, the same result can be obtained from the characteristic function under resetting times drawn from a PDF with finite moments. To do this, we need to consider the long time limit. Since the functionals we are considering here are additive, Z grows with t, so we can expect Z to be of the order of t, which means that s and p are comparable. Therefore, the long time limit corresponds to assuming that s and s are both small and comparable.

Writing $Q(p, t|x_0)_0$ as a moment-generating function

$$Q(p, t|x_0)_0 = \sum_{n=0}^{\infty} \frac{(-p)^n}{n!} \langle Z(t|x_0)_0^n \rangle,$$

one can see that

$$\mathcal{L}_{t\to s}[\varphi(t)Q(p,t|x_0)_0]$$

$$=\sum_{n=0}^{\infty} \frac{(-p)^n}{n!} \int_0^{\infty} e^{-st} \varphi(t) \langle Z(t|x_0)^n \rangle_0 dt,$$

and analogously $\mathcal{L}_{t\to s}[\varphi^*(t)Q(p,t|x_0)_0]$. Considering the limit $p\to 0$ to the above expression, the approximations

$$\mathcal{L}_{t\to s}[\varphi(t)Q(p,t|x_0)_0]$$

$$= \varphi(s) - p \int_0^\infty e^{-st} \varphi(t) \langle Z(t|x_0) \rangle_0 dt + O(p^2)$$

and

$$\mathcal{L}_{t \to s}[\varphi(t)^* Q(p, t | x_0)_0]$$

$$= \varphi^*(s) - p \int_0^\infty e^{-st} \varphi^*(t) \langle Z(t | x_0) \rangle_0 dt + O(p^2)$$

hold if

$$\lim_{s \to 0} \int_0^\infty e^{-s\tau} \varphi(\tau) \langle Z(\tau | x_0)^n \rangle_0 d\tau < \infty \tag{32}$$

for any $n \in \mathbb{N}$. This condition is necessary to guarantee that all the coefficients of the expansion in powers of p are finite when taking the limit $s \to 0$. Thus, from Eq. (10)

$$\tilde{Q}(p, s|x_0)_r \simeq \frac{\varphi^*(s)}{1 - \varphi(s) + p \int_0^\infty e^{-st} \varphi(t) \langle Z(t|x_0) \rangle_0 dt}
= \frac{1}{s + p\mathcal{I}(s)},$$
(33)

as $p \to 0$, where

$$\mathcal{I}(s) = \frac{s}{1 - \varphi(s)} \int_0^\infty e^{-st} \varphi(t) \langle Z(t|x_0) \rangle_0 dt.$$
 (34)

If the resetting times PDF has finite moments, then $\varphi(s) \simeq 1 - \langle t \rangle_R s + ...$ as $s \to 0$, then condition (32) is always satisfied, as can be shown using the same arguments to find Eq. (27). Hence, $\lim_{s\to 0} \mathcal{I}(s) = \mathcal{I}$ where

$$\mathcal{I} = \frac{1}{\langle t \rangle_R} \int_0^\infty \varphi(\tau) \langle Z(\tau|x_0) \rangle_0 d\tau.$$

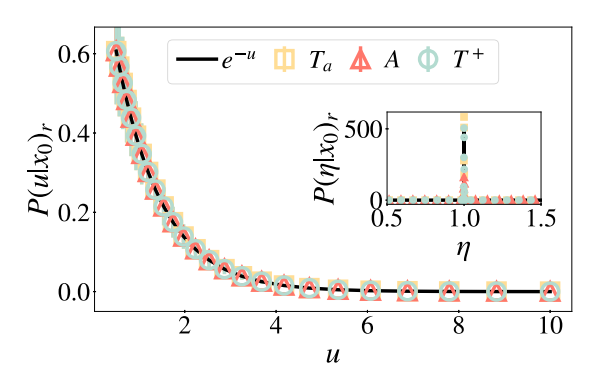


FIG. 1. Limiting PDF of observable Z for exponentially distributed resetting of three observables in Laplace space. The black line represents the Laplace transform of Eq. (31) and the symbols are obtained from the Laplace transform of the results of Monte Carlo simulations. In yellow squares $Z=T_a$ with a=1; in orange triangles Z=A, and in light-blue circles $Z=T^+$. In the inset we represent the same data in η space. For all simulations: $x_0=0$, D=1, $\langle t \rangle_R=1.2$ with $\varphi(t)=e^{-t/\langle t \rangle_R}/\langle t \rangle_R$. All simulations are run for $N=10^5$ particles for a total simulation time of $t=10^7$ with a time discretization of dt=0.1. The data points are plotted with their error bars.

Finally, performing the double Laplace inversion of Eq. (33) with respect to p and s we get

$$P(Z, t|x_0)_r = \delta(Z - \mathcal{I}t),$$

which is exactly Eq. (30) provided that $\langle Z(t|x_0)\rangle_r \simeq \mathcal{I}t$ from Eq. (28). In terms of the variable $\eta = Z/\mathcal{I}t$ it reads $P(\eta|x_0)_r = \delta(\eta - 1)$ as Eq. (31). This constitutes the first general result of this work.

From the derivation above, we see that any positive functional of a random walk in the presence of stochastic resetting is ergodic, provided that the PDF of resetting times has finite moments. Thus, for sufficiently long times, the PDF of the functional $P(Z, t|x_0)_r$ tends to a delta centered on the mean value. In Fig. 1 we check the results for the limiting PDF of three observables: (i) the occupation time inside the interval [-a, a], $T_a = \int_0^t \theta(-a < x(\tau) < a)d\tau$, (ii) the area under the square position $A = \int_0^{\tau} x^2(\tau) d\tau$ (this functional has been studied when the underlying motion is subdiffusive and without resetting [24]), and (iii) the half occupation time $T^+ = \int_0^t \theta(x(\tau))d\tau$, for exponentially distributed resets. We have conducted Monte Carlo simulations to compute the PDF of the observables when the underlying random walk is a Brownian motion, details on the simulations can be found in Appendix B. We compare the data with the theoretical prediction in the Laplace space, in which $P(u|x_0)_r =$ $\int_0^\infty e^{-u\eta} P(\eta|x_0)_r d\eta = e^{-u}$. As can be seen in the figure, the three functionals T_a , A, and T^+ collapse on the theoretical line, which proves that our theoretical result given in Eq. (30) holds for any positive functional.

B. Moments in the long-time limit

We can obtain the temporal dependence of the first two moments $\langle Z(t|x_0)\rangle_r$ and $\langle Z(t|x_0)^2\rangle_r$ in the long-time limit. To do this, we again assume that $\langle Z(t|x_0)\rangle_0 \sim t^{\mu}$ with $\mu > 0$, as $t \to \infty$. Let us consider that the resetting times are drawn

TABLE I. Top: long-time limit behavior of the two first moments for $0 \le \mu \le 1$. Bottom: long-time limit behavior of the two first moments for $1 < \mu \le 2$.

α	$\langle Z(t x_0)\rangle_r$	$\langle Z(t x_0)^2 \rangle_r$
$0 < \alpha \leqslant \mu$	$\sim t^{\mu}$	$\sim t^{2\mu}$
$\mu < \alpha \leqslant 1$	$\sim t^{\alpha}$	$\sim t^{2\alpha}$
$1 < \alpha \leqslant 2$	$\sim t$	$\sim t^2$
α	$\langle Z(t x_0)\rangle_r$	$\langle Z(t x_0)^2\rangle_r$
$0 < \alpha \leqslant 1$	$\sim t^{\mu}$	$\sim t^{2\mu}$
$1 < \alpha \leqslant \mu$	$\sim t^{1+\mu-lpha}$	$\sim t^{1+2\mu-\alpha}$

from a fat-tailed PDF $\varphi(t) \sim t^{-1-\alpha}$ with $0 < \alpha \le 2$. The moments of this PDF are diverging if $0 < \alpha < 1$, but the first moment is finite if $1 < \alpha < 2$. In particular, let us consider that the resetting time PDF follows the fat-tailed density

$$\varphi(t) = \frac{\alpha t_0^{\alpha}}{t^{1+\alpha}}, \quad t > t_0, \tag{35}$$

and 0 otherwise. Note that the limit $\alpha \to 0$ here corresponds to the absence of resetting because in this limit $\varphi \to 0$ and $\varphi^* \to 1$. To compute the long-time limit we need to consider $s \to 0$ in Eqs. (14) and (15). To do this we need to deal with integrals of the form (see Chapter 13 of Ref. [36])

$$\int_{t_0}^{\infty} e^{-st} t^{\beta} dt = t_0^{\beta+1} e^{-st_0} U(1, 2+\beta, st_0), \tag{36}$$

where U(a, b, z) is the Kummer U function. In the limit $st_0 \ll 1$ this function can be approximated to find (see Appendix A for details)

$$\int_{t_0}^{\infty} e^{-st} t^{\beta} dt \sim \begin{cases} \operatorname{const}, & \beta < -1 \\ s^{-1-\beta}, & \beta > -1. \end{cases}$$

Hence, the terms in Eqs. (14) and (15) follow as

$$\mathcal{L}_{t\to s}[\varphi(t)\langle Z(t|x_0)^n\rangle_0]$$

$$\sim \int_{t_0}^{\infty} e^{-st} t^{n\mu-1-\alpha} dt \sim \begin{cases} \text{const}, & \alpha > n\mu \\ s^{\alpha-n\mu}, & \alpha < n\mu, \end{cases}$$

and

$$\mathcal{L}_{t \to s} [\varphi^*(t) \langle Z(t|x_0)^n \rangle_0]$$

$$\sim \int_{t_0}^{\infty} e^{-st} t^{n\mu - \alpha} dt \sim \begin{cases} \text{const}, & \alpha > 1 + n\mu \\ s^{\alpha - n\mu - 1}, & \alpha < 1 + n\mu. \end{cases}$$

Keeping only the dominant terms in Eqs. (14) and (15), we obtain the results in Table I. Note that the scaling exponent of the moments depends on the values of the exponents α and μ . This is the second general result of this work, where we find the long-time behavior of the first two moments of a functional with fat-tailed resetting in terms of the temporal scaling of the moments of the functional without resetting.

For the particular case where Z corresponds to the occupation time in an interval T_a , in the absence of resetting, i.e., for free Brownian motion, $\langle T_a(t)\rangle_0 \sim t^{1/2}$ and $\langle T_a^2(t)\rangle_0 \sim t$ and

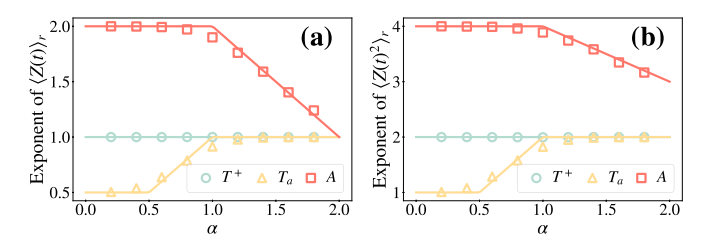


FIG. 2. Exponent ν (of $\sim t^{\nu}$) of (a) and (b) moments of the observables T^+ , T_a , and A for a Brownian walker with fat-tailed resetting [Eq. (35)] as a function of the resetting exponent α . For every value of α , we have computed the values of the observables for the simulation times $t = \{10^3, 10^4, 10^5, 10^6, 10^7\}$. Then, we have performed a least-squares fit to $\log_{10}(\langle Z(t)^{1.2} \rangle_r) = \nu \log_{10}(t) + c$, the symbols in the plots represent the obtained values of ν . The solid lines are obtained from Table I. For all simulations, the parameters used are: a time discretization of dt = 0.1, D = 1, and $t_0 = 1$ for the resetting PDF, the points for $\alpha = 0.2$, 1.8 are run for $N = 10^6$ particles, and all the rest for $N = 10^5$.

so $\mu = 1/2$. The results in Table I predict

$$\langle T_a(t) \rangle_r \sim \begin{cases} t^{1/2}, & 0 < \alpha \leqslant 1/2 \\ t^{\alpha}, & 1/2 \leqslant \alpha < 1 \end{cases}$$

$$\langle T_a^2(t) \rangle_r \sim \begin{cases} t, & 0 < \alpha \leqslant 1/2 \\ t^{2\alpha}, & 1/2 \leqslant \alpha < 1 \end{cases}$$

in agreement with Eqs (118) and C15 in Ref. [28].

In Fig. 2 we check the results shown in Table I for the three different stochastic functionals considered in Fig. 1: T_a , T^+ , and A. The agreement is excellent.

V. APPLICATION: HALF OCCUPATION TIME

In Ref. [28] we studied the statistical properties of the occupation time in an interval T_a , using the backward recurrence time to compute the renewal equation for the PDF of T_a . In this section, we apply the previous general results to the case of the half occupation time:

$$T^{+}(t|x_0) = \int_0^t \theta[x(\tau)]d\tau, \tag{37}$$

which is a measure of the time spent by the walker in x > 0 along the temporal window [0, t].

A. The two first moments and EB

In the absence of resetting the mean and the mean square half occupation time of the Brownian motion are $\langle T^+(t|x_0)\rangle_0 = t/2$ and $\langle T^+(t|x_0)^2\rangle_0 = 3t^2/8$. If we consider the fat-tailed resetting density in Eq. (35) and using Eq. (36) together with (14) and (15) we obtain (see Appendix C for details)

$$\langle T^{+}(t|x_{0})\rangle_{r} \simeq \frac{t}{2},$$

$$\langle T^{+}(t|x_{0})^{2}\rangle_{r} \simeq \begin{cases} \frac{3-\alpha}{8}t^{2}, & 0 < \alpha < 1\\ \frac{1}{4}t^{2}, & 1 < \alpha < 2 \end{cases}$$
(38)

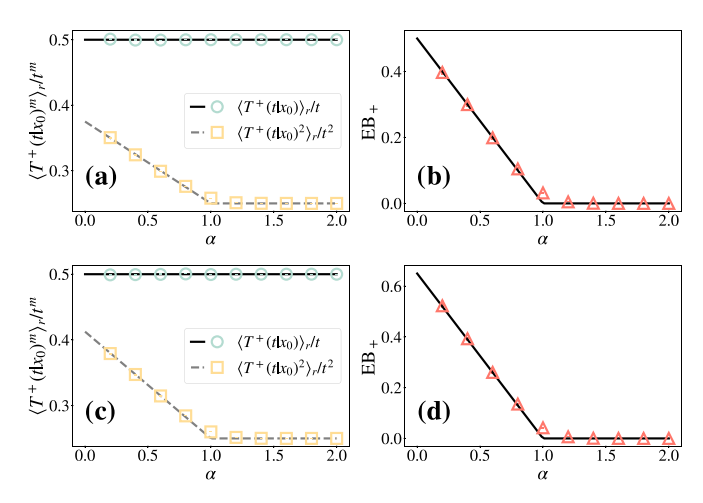


FIG. 3. (a) Mean (m = 1) and mean square (m = 2) half occupation time of a Brownian motion with fat-tailed resetting [Eq. (35)] over the m-th power of the total simulation time t as a function of the resetting exponent α . The solid black line and the dashed gray line represent Eq. (38) over t and t^2 , respectively. The symbols are obtained from Monte Carlo simulations, the light-blue circles represent the mean half occupation time over t; and the yellow squares represent the mean square half occupation time over t^2 . (b) The EB parameter for T^+ as a function of the resetting exponent α . The solid black line represents Eq. (39) and the orange triangles are obtained from the same Monte Carlo simulations used in (a). (c) and (d) Represent the same analysis but for a subdiffusive walker with fat-tailed resetting. In these figures the lines correspond to Eq. (40) in (c), and Eq. (41) in (d). The symbols are obtained from Monte Carlo simulations of a CTRW. For all simulations, the parameters used are: $x_0 = 0$, and $t_0 = 1$ for the resetting PDF. For (a) and (b) D = 1, and dt = 0.1 and for (c) and (d) the waiting time PDF has $t_{\gamma,0} = 1$, and $\gamma = 0.7$, and the jump PDF $\sigma = 0.01$. All simulations are run for $N = 10^5$ particles for a total simulation time of $t = 10^7$. The data points are plotted with their error bars.

in the long-time limit. Now, from (22) the EB parameter easily follows:

$$EB_{+} = \begin{cases} \frac{1-\alpha}{2}, & 0 < \alpha < 1\\ 0, & 1 < \alpha < 2 \end{cases}$$
 (39)

Equations (38) and (39) are the third result of this work. Note that this result predicts an ergodic transition between nonergodic and ergodic phases at $\alpha=1$. For $1<\alpha<2$ the observable $\theta[x(\tau)]$ is ergodic, which is in agreement with the fact that for these values of α the resetting times PDF has the first moment finite and the limiting PDF for T^+ converges to the delta function. Note that the condition that the resetting time PDF has to have finite moment can be actually relaxed to require that only the first moment must be finite in this case. For $0<\alpha<1$ the resetting times PDF has infinite moments, the observable is nonergodic, and the limiting PDF converges towards a *generalized arcsine law* as we show below. Note that for $\alpha=0$ one has EB₊ = 1/2, which corresponds to the value of EB₊ in the absence of resetting.

It is interesting to note that the presence of resetting reduces the value of EB_+ to such an extent that if the resetting is frequently enough (in particular, if $\alpha > 1$) the observable becomes ergodic. In Figs. 3(a) and 3(b) we compare

Eqs. (38) and (39) with numerical simulations. The agreement is excellent.

Let us now consider that the walker moves subdiffusively. In this case, for a Brownian motion without resetting the two first moments of the half occupation time are $\langle T^+(t|x_0)\rangle_0 = t/2$ and $\langle T^+(t|x_0)^2\rangle_0 = (4-\gamma)t^2/8$, where γ is the exponent of the power-law PDF of waiting times of the walker [37]. Considering the fat-tailed resetting PDF given in Eq. (35) then, using (36), we have

$$\langle T^{+}(t|x_{0})\rangle_{r} \simeq \frac{t}{2},$$

$$\langle T^{+}(t|x_{0})^{2}\rangle_{r} \simeq\begin{cases} \frac{4-\gamma-\alpha(2-\gamma)}{8}t^{2}, & 0 < \alpha < 1\\ \frac{1}{4}t^{2}, & 1 < \alpha < 2 \end{cases}$$
(40)

in the long-time limit. Now, from Eq. (22) the EB parameter easily follows:

$$EB_{+} = \begin{cases} \frac{(1-\alpha)(2-\gamma)}{2}, & 0 < \alpha < 1\\ 0, & 1 < \alpha < 2 \end{cases}$$
 (41)

Equations (40) and (41) are the fourth result of this work. For $\gamma=1$ the walker moves diffusively and Eq. (41) reduces to Eq. (39) as expected. In addition, the transition to the ergodic phase is determined by the values of α for which the resetting PDF has finite first moment, i.e., it occurs again at $\alpha=1$. We proceed in an analogous way than for the diffusive case, and in Figs. 3(c) and 3(d) we compare the predictions from Eqs. (40) and (41) with Monte Carlo numerical simulations. For the subdiffusive walker, we have simulated a Continuous Time Random Walk (CTRW) with a jump PDF of $\Psi(x)=\frac{\delta(x+\sigma)}{2}+\frac{\delta(x-\sigma)}{2}$ and a power-law waiting time PDF of parameter γ : $\varphi(t)=\gamma t_{\gamma,0}^{\gamma}t^{-1-\gamma}$, $t>t_{\gamma,0}$ and 0 otherwise, $t_{\gamma,0}=1$. Again, we see a good agreement between the analytic predictions and the simulations.

B. Limiting PDF

To compute the limiting PDF of Z in the presence of resetting, we start from its characteristic function $\tilde{Q}(p, s|x_0)_r$, which can be computed from Eq. (10). Assume that in the long-time limit the PDF $P(Z, t|x_0)_0$ has a scaling solution

$$\lim_{t \to \infty} P(Z, t | x_0)_0 = \frac{1}{t^{\beta}} f\left(\frac{Z}{t^{\gamma}}\right).$$

Then, the Laplace transform in the numerator of Eq. (10) can be written as

$$\mathcal{L}_{t\to s}[\varphi(t)Q(p,t|x_0)]$$

$$= \int_0^\infty dt \ e^{-st}\varphi(t) \int_0^\infty e^{-pZ} \frac{1}{t^\beta} f\left(\frac{Z}{t^\gamma}\right) dZ$$

$$= \int_0^\infty du \ f(u) \int_0^\infty e^{-st-put^\gamma} t^{\gamma-\beta}\varphi(t) dt, \qquad (42)$$

where we have introduced the new variable $u = Z/t^{\gamma}$. Note that the integral over time can be expressed as the Laplace transform of $\varphi(t)$ only if $\gamma = \beta = 1$. This is the case of the half occupation time, for which the PDF $P(T^+, t|x_0)_0$ has a limiting density of the form $\lim_{t\to\infty} P(T^+, t|x_0)_0 = f(T^+/t)/t$ for $0 < T^+ < t$. Two relevant examples are the

Lévy asrcsine [38] or the Lamperti [39] distributions which correspond to case where the underlying random walk is either normal diffusion or subdiffusion, respectively. In this case, $u = T^+/t$ and the Laplace transforms in Eq. (10) read

$$\mathcal{L}_{t\to s}[\varphi(t)Q(p,t|x_0)] = \int_0^1 f(u)\tilde{\varphi}(s+pu)du,$$

$$\mathcal{L}_{t\to s}[\varphi^*(t)Q(p,t|x_0)] = \int_0^1 f(u)\tilde{\varphi}^*(s+pu)du. \quad (43)$$

To proceed further, we consider the long time limit where s and p are both small and comparable. Since $u \in [0, 1]$, the argument s + pu is always small. Let us consider that the PDF of resettings has a power law fall-off with index α

$$\varphi(t) \sim t^{-1-\alpha}, \quad 0 < \alpha < 2$$
 (44)

as $t \to \infty$. It is not difficult to show that for $0 < \alpha < 1$ all the moments of φ are divergent, while if $1 < \alpha < 2$, only the first moment $\langle t_R \rangle = \int_0^\infty t \varphi(t) dt$ is finite. Using the Tauberian theorem [40], Eq. (44) admits the following expansion in Laplace space for small s:

$$\tilde{\varphi}(s) = \begin{cases} 1 - b_{\alpha} s^{\alpha} + \cdots, & 0 < \alpha < 1 \\ 1 - \langle t_R \rangle s + \cdots, & 1 < \alpha < 2, \end{cases}$$
(45)

where b_{α} depends on the details of the specific expression for $\varphi(t)$. With the help of (45), Eqs. (43) can be approximated as

$$\mathcal{L}_{t\to s}[\varphi(t)Q(p,t|x_0)]$$

$$\approx \begin{cases} 1 - b_{\alpha} \int_0^1 f(u)(s+pu)^{\alpha} du, & 0 < \alpha < 1 \\ 1 - \langle t_R \rangle \int_0^1 f(u)(s+pu) du, & 1 < \alpha < 2 \end{cases}$$

$$\mathcal{L}_{t\to s}[\varphi^*(t)Q(p,t|x_0)]$$

$$\approx \begin{cases} b_{\alpha} \int_0^1 f(u)(s+pu)^{\alpha-1} du, & 0 < \alpha < 1 \\ \langle t_R \rangle, & 1 < \alpha < 2. \end{cases}$$
(46)

Let us first consider the case $1 < \alpha < 2$. Plugging Eq. (46) into Eq. (10)

$$Q(p, s|x_0)_r \approx \frac{1}{\int_0^1 f(u)(s + pu)du} = \frac{1}{s + p\langle u \rangle},$$

where $\langle u \rangle = \int_0^1 u f(u) du$. Since $\langle u \rangle = \langle T^+ \rangle / t$, the double Laplace transform of $Q(p, s|x_0)_r$ with respect to p and s yields

$$P(T^{+}, t|x_{0})_{r} = \delta(T^{+} - \langle T^{+}(t|x_{0})\rangle_{r})$$
(47)

which is in agreement with Eq. (30).

Next, we consider the case $0 < \alpha < 1$. By setting Eq. (46) in Eq. (10) we readily obtain

$$Q(p, s|x_0)_r \approx \frac{\int_0^1 f(u)(s + pu)^{\alpha - 1} du}{\int_0^1 f(u)(s + pu)^{\alpha} du}.$$
 (48)

It is worth mentioning that this result establishes a link between the characteristic function of T^+ under a resetting with the limiting PDF of T^+ in absence of resetting assuming that the resetting PDF decays as $t^{-1-\alpha}$ for $0<\alpha<1$ as $t\to\infty$, regardless of the other details and structure of the resetting PDF. The characteristic function (48) can be rewritten in the

scaling form

$$Q(p, s|x_0)_r \approx \frac{1}{s} g_{\alpha} \left(\frac{p}{s}\right),$$

where

$$g_{\alpha}(\chi) = \frac{1}{\chi} \frac{\int_0^1 f(u)(\chi^{-1} + u)^{\alpha - 1} du}{\int_0^1 f(u)(\chi^{-1} + u)^{\alpha} du}$$
(49)

and $\chi = p/s$. The double Laplace inversion from p and s to T^+ and t has the form $P(T^+, t|x_0)_r \equiv P(z)_r$ where $z = T^+/t$. To find $P(z)_r$ we follow the method in Ref. [25] by noting

$$P(z)_r = -\frac{1}{\pi z} \lim_{\epsilon \to 0} \text{Im} \left[g_\alpha \left(-\frac{1}{z + i\epsilon} \right) \right]. \tag{50}$$

Calculating the imaginary part of Eq. (50) we find (see Appendix D for details)

$$P(z)_{r} = \frac{\sin(\alpha\pi)}{\pi} \times \frac{C_{\alpha}(z)C_{-1+\alpha}(1-z) + C_{-1+\alpha}(z)C_{\alpha}(1-z)}{C_{\alpha}(z)^{2} + 2C_{\alpha}(z)C_{\alpha}(1-z)\cos(\alpha\pi) + C_{\alpha}(1-z)^{2}},$$
(51)

with $z=T^+/t$ and $C_{\beta}(z)$ is given in Eq. (D2). Equation (51) is the fifth result of this work. Notably, this is the limiting PDF for T^+/t under resetting times sampled from a PDF with a tail that decays as $t^{-1-\alpha}$ with $0<\alpha<1$. This expression is general and holds for any underlying isotropic random walk. It can be explicitly found if the limiting PDF of T^+/t without resetting is known. It is important to stress that Eq. (51) holds when the resetting time PDF decays as a power law with an exponent such that all moments are divergent, this is, for $\alpha<1$. For $\alpha\geqslant 1$, the resetting times PDF has the first moment finite and, therefore, the limiting PDF is not given by Eq. (51) but by Eq. (30). Note that we have derived this result by using that scaling solution of the reset-free process is $\lim_{t\to\infty} P(Z,t|x_0)_0 = f(Z/t)/t$, therefore Eq. (51) will also hold for any other potential functional with the same scaling

$$C_{\alpha}\left(\frac{1}{2}\right)C_{\alpha-1}^{"}\left(\frac{1}{2}\right) - C_{\alpha}^{"}\left(\frac{1}{2}\right)C_{\alpha-1}\left(\frac{1}{2}\right) - 2C_{\alpha}^{'}\left(\frac{1}{2}\right)C_{\alpha-1}^{'}\left(\frac{1}{2}\right)$$

$$= 2\frac{C_{\alpha-1}\left(\frac{1}{2}\right)C_{\alpha}^{'}\left(\frac{1}{2}\right)}{C_{\alpha}\left(\frac{1}{2}\right)}\tan^{2}\left(\frac{\alpha\pi}{2}\right), \tag{52}$$

where the primes stand for derivatives with respect to z. This equation has to be numerically solved once the analytic expression for $C_{\beta}(z)$ is calculated from Eq. (D2).

1. Brownian walker

If, for example, the underlying random walk is a Brownian motion then the limiting PDF of T^+/t without resetting obeys the Lévy arcsine law [38]

$$f(u) = \frac{1}{\pi \sqrt{u(1-u)}},$$
 (53)

if 0 < u < 1 and from (D2) with (53) we obtain

$$C_{\beta}(z) = \frac{\Gamma(1+\beta)}{\sqrt{\pi}\Gamma(\frac{3}{2}+\beta)} z^{\frac{1}{2}+\beta} {}_{2}F_{1}\left(\frac{1}{2}, \frac{1}{2}; \frac{3}{2}+\beta; z\right), \quad (54)$$

where ${}_2F_1(\cdot)$ is the Gauss's hypergeometric function. In the limit $u \to 0$, $f(u) \sim u^{-1/2}$ and from Eq. (54) we see that $C_{\beta}(z) \sim z^{\beta+1/2}$ as $z \to 0$. Hence, from Eq. (51)

$$P(z)_r \sim z^{\alpha - 1/2}, \quad z \to 0^+,$$

 $P(z)_r \sim (1 - z)^{\alpha - 1/2}, \quad z \to 1^-.$ (55)

As we can see from Eq. (55), when $\alpha > 1/2$, the most unlikely values of T^+ are 0 and t, which are given with vanishing probability. In this case, due to the symmetry of the random walk, the most likely value is $T^+ = t/2$, giving rise to a \cap shape limiting PDF. Then, a sufficiently frequent resetting induces the walker to spend an equal amount of time in the domain x > 0 and x < 0, in the long-time limit. Conversely, recall that for the case without resetting, the limiting PDF follows the Lévy's arcsine law, where the most probable values of T^+ are 0 and t, implying that a walker is mostly in the positive or negative domain for its entire trajectory. When α < 1/2, the resetting is less frequent and the probability of T^+ at 0 and t does not vanish anymore. In this regime, we can distinguish two possibilities: for a given value of α , say α_c , if $0 < \alpha < \alpha_c$ the limiting PDF has a \cup shape, as in the case without resetting, and the most likely values are $T^+ = 0$ or $T^+ = t$. On the other hand, if $\alpha_c < \alpha < 1/2$, the limiting PDF has the W shape and the most likely values are $T^+ = 0, T^+ = t$, and $T^+ = t/2$, as a transition between \cup and \cap shapes. The value of α_c can be found by solving Eq. (52) with Eq. (54). The resulting nonlinear equation for α has to be numerically solved. It solution yields $\alpha_c = 0.269$.

In Fig. 4 we compare Eq. (51) with Eq. (54) against Monte Carlo simulations conducted for three different resetting time PDFs which decay in time as $t^{-1-\alpha}$ in the long-time limit: power-law (PL) $\varphi(t) = \alpha t_0^{\alpha} t^{-1-\alpha}$, $t > t_0$ and 0 otherwise, $t_0 = 1$; Mittag-Leffler (ML) $\varphi(t) = t^{\alpha-1} \tau^{-\alpha} E_{\alpha,\alpha}(-t^{\alpha} \tau^{-\alpha})$ with $E_{\alpha,\beta}(\cdot)$ the two-parametric Mittag-Leffler function [41,42], $\tau = |\Gamma(1-\alpha)|^{1/\alpha}$; and Lévy (LV), where $\varphi(t) =$ $l_{\alpha}(t)$ is the one-sided Lévy stable distribution [43,44]. As can be seen, the limiting PDF (51) agrees with all three cases. This confirms that the limiting PDF depends only on the tail of the resetting times PDF. In addition, we have included the case of exponentially distributed resetting time together with the power-law PDF with $\alpha > 1$ [Fig. 4(d)]. In both cases, the resetting times PDF has a finite first moment, and the limiting PDF under resetting fits Eqs. (31). It is also interesting to observe the aforementioned transition of the three different shapes W, \cup , and \cap for different values of α .

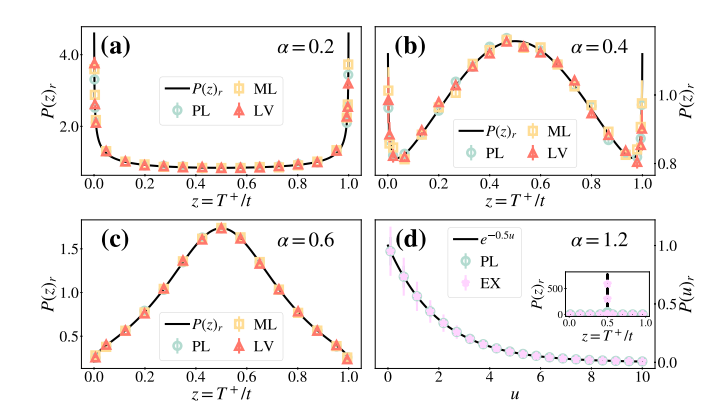


FIG. 4. Limiting PDF of the half occupation time of a Brownian Motion with resetting for a variety of resetting distributions. All symbols are obtained from Monte Carlo simulations of a Brownian walker with different resetting PDFs: power-law (PL) in light-blue circles with $t_0 = 1$; Mittag-Leffler (ML) in yellow squares; Lévy (LV) in orange triangles; and exponential (EX) in pink stars with $\langle t \rangle_R = t_0 \alpha (\alpha - 1)^{-1}$. In (a), (b), and (c) the solid black line represents Eq. (51) with the $C_\beta(z)$ coefficients obtained from Eq. (54). In (d) we present the Laplace transform of Eq. (47) $P(u)_r = \mathcal{L}_{z \to u}[P(z)_r]$. In the inset of (d) it is plotted in z space. For all simulations the parameters used are: $x_0 = 0$, D = 1, and parameter of the resetting distribution, $\alpha = 0.2$, 0.4, 0.6 and 1.2 for (a)–(d), respectively. All simulations are run for $N = 10^5$ particles for a total simulation time of $t = 10^7$ with a time discretization of dt = 0.1. The data points are plotted with their error bars.

2. Subdiffusive walker

When the underlying random walker performs a subdiffusive motion, then the limiting PDF in the absence of resetting is given by the Lamperti distribution [39]

$$f(u) = \frac{\sin(\gamma \pi/2)}{\pi} \frac{[u(1-u)]^{\frac{\gamma}{2}-1}}{u^{\gamma} + (1-u)^{\gamma} + 2[u(1-u)]^{\frac{\gamma}{2}} \cos(\gamma \pi/2)}.$$
(56)

Recall that the exponent γ is related to the index of fractional derivative, or alternatively, it is the exponent of the waiting time between jumps when its PDF decays as $t^{-1-\gamma}$ with $0 < \gamma < 1$ in the long-time limit. In this case, it is not possible to perform analytically the integral in Eq. (D2). However, we can unveil the behavior of Eq. (51) near z=0 and z=1. This will allow us to know for which value of α and γ the transition between the shapes \cup and W appears. Close to z=0 the Lamperti distribution (56) behaves as $f(u) \sim u^{\gamma/2-1}$ so that from (D2) we find $C_{\beta}(z) \sim z^{\beta+1/2}$. Hence,

$$P(z)_r \sim z^{\alpha + \frac{\gamma}{2} - 1}, \quad z \to 0^+,$$

 $P(z)_r \sim (1 - z)^{\alpha + \frac{\gamma}{2} - 1}, \quad z \to 1^-,$ (57)

Then, if $0 < \alpha < \alpha_c$ the PDF $P(z)_r$ has the \cup shape, if $\alpha_c < \alpha < \alpha^*$ it has the shape W where $\alpha^* = 1 - \gamma/2$, and for $\alpha^* < \alpha < 1$ it has the \cap shape. The transition between W and \cap shapes is attained at $\alpha = \alpha_c$ which has to be found as in the previous example. The transition at $\alpha^* = 1 - \gamma/2$ can be understood in terms of the First Passage Time (FPT) of the walker to reach the origin. If the FPT has a diverging mean, the walker stays either at x > 0 or x < 0, and therefore

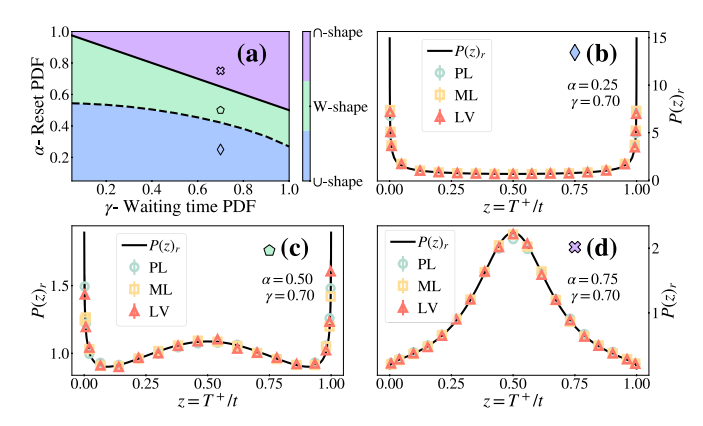


FIG. 5. (a) Phase diagram of the limiting PDF of T^+ of a subdiffusive walker with resetting of exponent α . The dashed line represents α_c and the solid line represents $\alpha^* = 1 - \gamma/2$. The black symbols mark the corresponding (γ, α) points represented in (b)–(d). (b)–(d) limiting PDF of T^+ for a subdiffusive walker with different resetting PDFs: power-law (PL) in light-blue circles with $t_0 = 1$; Mittag-Leffler (ML) in yellow squares; Lévy (LV) in orange triangles. The symbols are obtained from Monte Carlo simulations of a CTRW with $\sigma = 0.01$. The black lines are computed by numerical integration of Eq. (D2) with the $C_{\beta}(z)$ coefficients obtained from Eq. (56). For all simulations, the parameters of the resetting distribution are $\alpha = 0.25, 0.5,$ and 0.75 for (b)–(d), respectively. The parameters of the waiting time PDF for all cases are $t_{\nu,0} = 1$, and $\gamma = 0.7$. All simulations are run for $N = 10^5$ particles for a total simulation time of $t = 10^7$, and initial condition $x_0 = 0$. The data points are plotted with their error bars.

the limiting PDF of T^+ is nonvanishing at 0 and $t \in W$ shapes). On the other hand, when the mean of the FPT is finite, the walker crosses the origin at a finite time, then the probability of the limiting PDF of T^+ vanishes at 0 and t, i.e., its has a maximum (\cap shape). The transition between a finite and diverging mean for a CTRW with resets is known [7] and is precisely at $\alpha = 1 - \gamma/2$. The same reasoning is valid for the case of the diffusive walker, as in that case $\gamma = 1$. In Ref. [16] the authors find a transition at $\alpha = 1 - \gamma/2$ for the propagator of a subdiffusive walker under a power-law resetting to the initial condition. For sufficiently long times, they find that the propagator changes from being flat near the origin for $\alpha < 1 - \gamma/2$ to having a sharp peak at x = 0 with a heavy-tailed decay for larger x. This indicates that resets are frequent enough to create strong localization around the reset point x = 0, while still allowing significant excursions away from it. The resulting profile has no characteristic scale, reflecting the interplay between the underlying random walk and the reset dynamics, in agreement with the transition observed in the limiting PDF of the half-occupation time. This same reasoning can be applied to the case in the previous section of a Brownian walker with power-law resetting, since we have observed a similar transition at $\alpha = 1/2$ for the infinite densities of the process [28].

In Fig. 5(a) we present the phase diagram for the shapes of $P(z)_r$ in terms of the exponents α and γ . We also present the dependence of the curves α^* and α_c . In Figs. 5(b)–5(d) we show a comparison between the curves obtained by numerically integrating Eq. (D2) with the $C_{\beta}(z)$

coefficients obtained from Eq. (56) and numerical simulations of the CTRW. In the figure, we show an example for the three different cases: \cup shape, W shape, and \cap shape. In all three cases, we obtain a very good agreement for three resetting distributions: power-law, Mittag-Leffler, and Lévy. This again confirms that the limiting PDF only depends on the tail of the resetting times PDF, also for the subdiffusive case. We want to note that fine numerical precision is needed, especially as $z \to 0$, 1, to numerically integrate the limiting PDF. This is particularly relevant near the transition values of α_c and α^* .

This behavior under resetting is reminiscent of the effects seen when a confining potential is present. Resetting the walker's position to the origin has certain similarities with the presence of a confining potential centered at this point [11,45]. Both mechanisms give rise to a nonequilibrium steady state, a finite mean first passage time, depending on the properties of the resetting times PDF and the underlying random walk [14]. They also share some statistical properties of certain stochastic functionals. For example, as we have seen above, the limiting PDF of T^+ has the \cup shape depending on the value of α . The same happens when the random walker moves in the presence of a force field [46]. The similarity, however, does not extend to the W shape or ∩ shape, which do not appear under a confining potential. Nevertheless, the transition between the shapes ∪ and W has been already found when a subdiffusive particle moves in a finite symmetric interval [24] or when a Brownian particle moves in a heterogeneous media [47].

VI. CONCLUSIONS

In this work, we have derived the characteristic function of functionals of random walk when its position is reset to the origin at random times sampled from a general PDF. We have derived the temporal scaling dependence of the first two moments of any stochastic functional of any random walk in the long-time limit when the resetting PDF has a power-law tail.

We have shown that the limiting PDF for any stochastic functional converges to a delta function centered at the mean value when the resetting PDF has finite moments. This implies that any functional is ergodic in the presence of exponential resetting, revealing the role of Poisonian resetting as an ergodicity-induced mechanism. We have further analyzed the ergodic properties of observables and have derived an expression for the EB parameter. In particular, we have computed the EB parameter for the half occupation time of Brownian and subdiffusive walkers under resetting times drawn from a power-law PDF, showing the existence of a transition between nonergodic and ergodic phases depending on the values of the exponent of the resetting distribution. In all cases, we have found that the EB+ parameter is smaller in the presence of resetting than for the reset-free system, revealing that in this case resetting also promotes ergodicity. Additionally, we have seen that for T^+ , the condition on the resetting PDF can be relaxed to require only a finite first moment for the limiting PDF to converge to a delta function, and we expect, though have not proved, that this relaxation could be extended to other functionals if the first moment without resetting scales as t^{μ} with $0 < \mu < 1$ in the long-time limit.

We have derived a general expression for the limiting PDF of any functional of an isotropic random walk under a power-law resetting PDF if the limiting PDF in absence of resetting satisfies $\lim_{t\to\infty} P(Z,t|x_0)_0 = f(Z/t)/t$. In particular, we have analyzed the half occupation time statistics. We have studied the specific cases of Brownian and subdiffusive underlying random walks and have shown the existence of different shapes of the limiting PDF: \cup , W, and \cap . The transition between the three shapes of the limiting PDF reveals the different behaviors of the system. The \cup shape is reminiscent of the reset-free system, and Lévy's arcsine law, where the walker spends most of its time either in the positive or the negative region. On the contrary, a \cap PDF reveals that resetting induces the walker to statistically be half of the time on the positive axis and half on the negative. Unlike the cases where the walker moves in the presence of a confining potential or in a heterogeneous medium, if it is subjected to a reset whose PDF decays as a power law, a transition between the W and \cap shapes appears. The study of the transition has allowed us to describe the confining role of the reset, which forces the walker to frequently revisit a region close to the origin, and affects the statistical properties of the half-occupation time. These insights provide a foundation for broader applications. The general expressions derived in this work can be applied to other functionals of interest, such as the time-averaged position or the area under the trajectory.

ACKNOWLEDGMENTS

The authors acknowledge the financial support of the Ministerio de Ciencia, Innovación y Universidades (Spanish government) under Grant No. PID2021-122893NB-C22.

DATA AVAILABILITY

The data that support the findings of this article are not publicly available upon publication because it is not technically feasible and/or the cost of preparing, depositing, and hosting the data would be prohibitive within the terms of this research project. The data are available from the authors upon reasonable request.

APPENDIX A: KUMMER FUNCTION FOR SMALL ARGUMENT

In this Appendix we illustrate the expansion of the Kummer U function (also known as confluent hypergeometric function or simply Tricomi's function) U(a, b, z) is defined as [36]

$$U(a, b, z) = \frac{\Gamma(1-b)}{\Gamma(1+a-b)} M(a, b, z) + \frac{\Gamma(b-1)}{\Gamma(a)} z^{1-b} M(a+1-b, 2-b, z), \quad (A1)$$

where

$$M(a,b,z) = \frac{\Gamma(b)}{\Gamma(a)} \sum_{n=0}^{\infty} \frac{\Gamma(a+n)}{\Gamma(b+n)} \frac{z^n}{n!}$$
 (A2)

is the Kummer M function. We are interested specifically in the case a=1. Inserting the series expansion (A2) into (A1) we can obtain the series expansion for U(a,b,z). Thus, depending on the values of b the leading terms in the limit $z \ll 1$ are

$$U(1, b, z) = \begin{cases} \frac{1}{1-b} + \frac{z}{b(1-b)} + \cdots, & b < 0, \\ \frac{1}{1-b} - \frac{\Gamma(b)}{1-b} z^{1-b} + \cdots, & 0 < b < 1, \\ \frac{\Gamma(b-1)}{z^{b-1}} + \cdots, & b > 1. \end{cases}$$
(A3)

APPENDIX B: NUMERICAL SIMULATIONS

In this Appendix, we outline the simulation algorithm which has been used to collect the data. All numerical simulations are based on Monte Carlo simulations of N particle trajectories. To simulate a single step of the random walk process for a given particle, we compute the time increment τ_i and the space increment Δ_i . For the Brownian motion $\tau_i = dt$ and $\Delta_i = \sqrt{2Ddt}\xi$ where dt is a time discretization constant, D is the diffusion coefficient, and ξ is a normal random variable N(0,1). On the other hand, for a CTRW the time and space increments are given by its Waiting Time PDF and the Jump Length PDF. In this work, we have worked with a jump length PDF of $\Psi(x) = \frac{\delta(x+\sigma)}{2} + \frac{\delta(x-\sigma)}{2}$ and a power-law waiting time PDF of parameter γ : $\phi(t) = \gamma t_{\gamma,0}^{\gamma} t^{-1-\gamma}$, $t > t_{\gamma,0}$ and 0 otherwise, with $t_{\gamma,0} = 1$. Then, $\tau_i = \frac{t_{\gamma,0}}{(1-u_1)^{1/\gamma}}$ and $\Delta_i = \text{sign}(u_2)\sigma$ where u_j are uniform random variables in the interval [0,1], and σ is a constant space discretization parameter.

Next, we need to compute the time τ^r when the resetting processes occur from the resetting PDF $\varphi(t)$. In this work we have considered the reset PDF to be EX $\varphi(t) = e^{-t/\langle t \rangle_R}/\langle t \rangle_R$; PL $\varphi(t) = \alpha t_0^\alpha t^{-1-\alpha}$, $t > t_0$ and 0 otherwise, $t_0 = 1$; ML $\varphi(t) = t^{\alpha-1}\tau^{-\alpha}E_{\alpha,\alpha}(-t^\alpha\tau^{-\alpha})$ with $E_{\alpha,\beta}(\cdot)$ the two-parametric ML function, $\tau = |\Gamma(1-\alpha)|^{1/\alpha}$; and LV, where $\varphi(t) = l_\alpha(t)$ is the one-sided Lévy stable distribution. The generation of random numbers from the exponential and power-law distributions is based on the cumulative probability function. For details on the ML random number generation, see Ref. [42] and for one-sided Lévy stable random numbers see Ref. [44].

To compute the time evolution of a single particle, we initialize the particle's position at $x=x_0$ and t=0 and compute the first resetting time τ_1^r , and perform M_1 random walk steps so that the position x and evolution time t are $x=x_0+\sum_{i=1}^{M_1}\Delta_i$ and $t=\sum_{i=1}^{M_1}\tau_i$ until $t=\tau_1^r$ is reached. Then the reset occurs meaning that walker's position is set to the initial position x_0 , a new resetting time τ_2^r is drawn from $\varphi(t)$ and the process starts anew, where now $x=x_0+\sum_{i=1}^{M_2}\Delta_i$ and $t=\sum_{i=1}^{M_1}\tau_i+\sum_{i=1}^{M_2}\tau_i$ until the next reset time τ_2^r is reached. This process is repeated until the maximum simulation time t_{\max} is attained, for which $M=\sum_l M_l$ steps have been performed. We note that we need to ensure that $\sum_{i=1}^{M_l}\tau_i=\tau_l^r$ so that the 1-th reset happens exactly at time τ_l^r . Therefore, we need to check that $\tau_{l,1}\leqslant \tau_l^r$, $\tau_{l,1}+\tau_{l,2}\leqslant \tau_l^2$,... for all time increments. When M_l-1 time increments are computed so that $\sum_{i=1}^{M_l-1}\tau_i\leqslant \tau_l^r$ and the next time increment τ_{M_l} is

such that $\sum_{i=1}^{M_l} \tau_i > \tau_l^r$ then time increment used is $\tau_{M_l} = \tau_l^r - \sum_{i=1}^{M_l-1} \tau_i$. The same procedures is considered in order to stop the simulation at exactly $t = t_{\text{max}}$. To compute the observables we consider $T_a = \sum_{i=1}^M t_i \theta(a - |x_i|)$, where is the total steps done in the simulation; $T^+ = \sum_{i=1}^M t_i \theta(x_i) + T_0/2$ where T_0 the time spent by the walker exactly at x = 0; and $A = \sum_{i=1}^M x_i^2 t_i$, where x_i is the position of the walker at the step i. We repeat this procedure over N realizations to compute the ensemble averages.

APPENDIX C: DERIVATION OF EQ. (38)

We consider the fat-tailed resetting density in Eq. (35) and use Eq. (36) to have

$$\mathcal{L}_{t\to s}[\varphi(t)\langle T^+(t|x_0)\rangle_0] = \frac{\alpha t_0}{2}e^{-st_0}U(1,2-\alpha,st_0)$$

and

$$\mathcal{L}_{t\to s}[\varphi^*(t)\langle T^+(t|x_0)\rangle_0]$$

$$= \frac{1 - (1 + st_0)e^{-st_0}}{2s^2} + \frac{t_0^2}{2}e^{-st_0}U(1, 3 - \alpha, st_0).$$

Analogously,

$$\mathcal{L}_{t\to s}[\varphi(t)\langle T^+(t|x_0)^2\rangle_0] = \frac{3\alpha t_0^2}{8}e^{-st_0}U(1, 3-\alpha, st_0)$$

and

$$\mathcal{L}_{t\to s}[\varphi^*(t)\langle T^+(t|x_0)^2\rangle_0]$$

$$= \frac{3}{8} \int_0^{t_0} e^{-st} t^2 dt + \frac{3t_0^3}{8} e^{-st_0} U(1, 4 - \alpha, st_0).$$

In the long-time limit we have to consider $st_0 \ll 1$ in the previous expressions by using the small argument approximation of the Kummer U function U(a, b, z). Making use of the results derived in Appendix A we thus find

$$\mathcal{L}_{t\to s}[\varphi(t)\langle T^{+}(t|x_{0})\rangle_{0}] \sim \frac{\alpha t_{0}}{2} \begin{cases} \frac{\Gamma(1-\alpha)}{(st_{0})^{1-\alpha}}, & 0 < \alpha < 1\\ \frac{1}{\alpha-1}, & 1 < \alpha < 2, \end{cases}$$

$$\mathcal{L}_{t\to s}[\varphi^{*}(t)\langle T^{+}(t|x_{0})\rangle_{0}] \sim \frac{t_{0}^{2}}{2} \frac{\Gamma(2-\alpha)}{(st_{0})^{2-\alpha}}, & 0 < \alpha < 2,$$

$$\mathcal{L}_{t\to s}[\varphi(t)\langle T^{+}(t|x_{0})^{2}\rangle_{0}] \sim \frac{3\alpha t_{0}^{2}}{8} \frac{\Gamma(2-\alpha)}{(st_{0})^{2-\alpha}}, & 0 < \alpha < 2,$$

$$\mathcal{L}_{t\to s}[\varphi^{*}(t)\langle T^{+}(t|x_{0})^{2}\rangle_{0}] \sim \frac{3t_{0}^{3}}{8} \frac{\Gamma(3-\alpha)}{(st_{0})^{3-\alpha}}, & 0 < \alpha < 3.$$

Finally, from Eqs. (14), (15), and the previous results, we obtain Eq. (38).

APPENDIX D: DERIVATION OF EQ. (51)

To compute the imaginary part in Eq. (50) we set $\chi^{-1} = -z - i\epsilon$ into the integrals of Eq. (49) and rewrite them as

$$\int_0^1 f(u)(\chi^{-1} + u)^{\alpha - 1} du = \int_0^1 f(u)(\epsilon^2 + (u - z)^2)^{\frac{-1 + \alpha}{2}} \cos[(-1 + \alpha)\theta(z, u, \epsilon)] du$$
$$+ i \int_0^1 f(u)(\epsilon^2 + (u - z)^2)^{\frac{-1 + \alpha}{2}} \sin[(-1 + \alpha)\theta(z, u, \epsilon)] du$$

and

$$\int_0^1 f(u)(\chi^{-1} + u)^{\alpha} du = \int_0^1 f(u)(\epsilon^2 + (u - z)^2)^{\frac{\alpha}{2}} \cos[\alpha \theta(z, u, \epsilon)] du + i \int_0^1 f(u)(\epsilon^2 + (u - z)^2)^{\frac{\alpha}{2}} \sin[\alpha \theta(z, u, \epsilon)] du,$$

where

$$\theta(z, u, \epsilon) = \tan^{-1}\left(\frac{-\epsilon}{u - z}\right).$$

Since the integration variable u ranges from 0 to 1 the angle $\theta(z, u, \epsilon)$ may take different values in the limit $\epsilon \to 0$. In particular, if $u \in [0, z]$ then $\lim_{\epsilon \to 0} \theta(z, u, \epsilon) = \pi$ while if $u \in [z, 1]$ then $\lim_{\epsilon \to 0} \theta(z, u, \epsilon) = 2\pi$. Consequently, the above integrals have to be split in performing the limit $\epsilon \to 0$. Taking the imaginary part of Eq. (49) using the previous integrals we find

$$\operatorname{Im} g_{\alpha}(z,\epsilon) = \frac{A_{-1+\alpha}(zB_{\alpha} - \epsilon A_{\alpha}) - B_{-1+\alpha}(zA_{\alpha} + \epsilon B_{\alpha})}{A_{\alpha}^{2} + B_{\alpha}^{2}},$$

where

$$A_{\beta} = \int_0^1 f(u) [\epsilon^2 + (u - z)^2]^{\frac{\beta}{2}} \cos[\beta \theta(z, y, \epsilon)] du$$

and

$$B_{\beta} = \int_0^1 f(u) [\epsilon^2 + (u - z)^2]^{\frac{\beta}{2}} \sin[\beta \theta(z, u, \epsilon)] du.$$

Next, we perform the limit $\epsilon \to 0$ to the expressions for A_{β} and B_{β} . We thus find

$$\lim_{\epsilon \to 0} \operatorname{Im} g_{\alpha}(z, \epsilon) = z \frac{\mathcal{A}_{-1+\alpha} \mathcal{B}_{\alpha} - \mathcal{B}_{-1+\alpha} \mathcal{A}_{\alpha}}{\mathcal{A}_{\alpha}^{2} + \mathcal{B}_{\alpha}^{2}}, \tag{D1}$$

where

$$\mathcal{A}_{\beta} = C_{\beta}(z)\cos(\beta\pi) + D_{\beta}(z)\cos(2\beta\pi),$$

$$\mathcal{B}_{\beta} = C_{\beta}(z)\sin(\beta\pi) + D_{\beta}(z)\sin(2\beta\pi)$$

and

$$C_{\beta}(z) = \int_{0}^{z} f(u)(z - u)^{\beta} du = z^{\beta + 1} \int_{0}^{1} f(zv)(1 - v)^{\beta} dv,$$

$$D_{\beta}(z) = \int_{z}^{1} f(u)(u - z)^{\beta} du,$$
(D2)

where we have introduced the new variable v = u/z. If the underlying random walk is isotropic then f(u) = f(1 - u) and thus $D_{\beta}(z) = C_{\beta}(1 - z)$. Finally, from Eqs. (D1) and (D2) we readily find Eq. (51).

- M. R. Evans and S. N. Majumdar, Diffusion with stochastic resetting, Phys. Rev. Lett. 106, 160601 (2011).
- [2] M. R. Evans, S. N. Majumdar, and G. Schehr, Stochastic resetting and applications, J. Phys. A 53, 193001 (2020).
- [3] B. Żbik and B. Dybiec, Lévy flights and Lévy walks under stochastic resetting, Phys. Rev. E 109, 044147 (2024).
- [4] M. Radice and G. Cristadoro, Optimizing leapover lengths of Lévy flights with resetting, Phys. Rev. E 110, L022103 (2024).
- [5] S. N. Majumdar, P. Mounaix, S. Sabhapandit, and G. Schehr, Record statistics for random walks and Lévy flights with resetting, J. Phys. A 55, 034002 (2022).
- [6] P. C. Bressloff, Occupation time of a run-and-tumble particle with resetting, Phys. Rev. E 102, 042135 (2020).
- [7] V. Méndez, A. Masó-Puigdellosas, T. Sandev, and D. Campos, Continuous time random walks under markovian resetting, Phys. Rev. E 103, 022103 (2021).
- [8] V. Méndez, R. Flaquer-Galmés, and D. Campos, First-passage time of a Brownian searcher with stochastic resetting to random positions, Phys. Rev. E 109, 044134 (2024).
- [9] N. Leibovich and E. Barkai, Infinite ergodic theory for heterogeneous diffusion processes, Phys. Rev. E 99, 042138 (2019).
- [10] G. Mercado-Vásquez, D. Boyer, and S. N. Majumdar, Freezing transitions of Brownian particles in confining potentials, J. Stat. Mech. Theory Exp. (2022) 063203.
- [11] M. R. Evans, S. N. Majumdar, and K. Mallick, Optimal diffusive search: Nonequilibrium resetting versus equilibrium dynamics, J. Phys. A 46, 185001 (2013).
- [12] S. Eule and J. J. Metzger, Nonequilibrium steady states of stochastic processes with intermittent resetting, New J. Phys. 18, 033006 (2016).
- [13] A. Chechkin and I. M. Sokolov, Random search with resetting: A unified renewal approach, Phys. Rev. Lett. 121, 050601 (2018).
- [14] A. Masó-Puigdellosas, D. Campos, and V. Méndez, Transport properties and first-arrival statistics of random motion with stochastic reset times, Phys. Rev. E 99, 012141 (2019).
- [15] V. P. Shkilev and I. M. Sokolov, Subdiffusive continuous time random walks with power-law resetting, J. Phys. A 55, 484003 (2022).

- [16] A. S. Bodrova and I. M. Sokolov, Continuous-time random walks under power-law resetting, Phys. Rev. E 101, 062117 (2020).
- [17] M. Kac, On distributions of certain Wiener functionals, Trans. Amer. Math. Soc. 65, 1 (1949).
- [18] M. Kac, On some connections between probability theory and differential and integral equations, in *Second Berkeley Symposium on Mathematical Statistics and Probability*, edited by J. Neyman (California University Press, Berkeley, 1951), pp. 189–215.
- [19] M. Yor, *Some Aspects of Brownian Motion*, Lectures in Mathematics, Eth Zürich (Birkhauser, Basel, 1992).
- [20] H. Geman and M. Yor, Bessel processes, asian options, and perpetuities, Math. Financ. 3, 349 (1993).
- [21] A. Comtet, J. Desbois, and C. Texier, Functionals of Brownian motion, localization and metric graphs, J. Phys. A 38, R341 (2005).
- [22] S. N. Majumdar, Brownian functionals in physics and computer science, *The Legacy of Albert Einstein* (Wiley, 2005), PP. 93–129.
- [23] L. Turgeman, S. Carmi, and E. Barkai, Fractional Feynman-Kac equation for non-Brownian functionals, Phys. Rev. Lett. 103, 190201 (2009).
- [24] S. Carmi, L. Turgeman, and E. Barkai, On distributions of functionals of anomalous diffusion paths, J. Stat. Phys. 141, 1071 (2010).
- [25] C. Godreche and J.-M. Luck, Statistics of the occupation time of renewal processes, J. Stat. Phys. 104, 489–524 (2001).
- [26] J. M. Meylahn, S. Sabhapandit, and H. Touchette, Large deviations for Markov processes with resetting, Phys. Rev. E **92**, 062148 (2015).
- [27] F. den Hollander, S. N. Majumdar, J. M. Meylahn, and H. Touchette, Properties of additive functionals of Brownian motion with resetting, J. Phys. A 52, 175001 (2019).
- [28] E. Barkai, R. Flaquer-Galmés, and V. Méndez, Ergodic properties of Brownian motion under stochastic resetting, Phys. Rev. E 108, 064102 (2023).

- [29] W. Wang, J. H. P. Schulz, W. Deng, and E. Barkai, Renewal theory with fat-tailed distributed sojourn times: Typical versus rare, Phys. Rev. E 98, 042139 (2018).
- [30] T. M. Michelitsch, G. D'Onofrio, F. Polito, and A. P. Riascos, Random walks with stochastic resetting in complex networks: A discrete-time approach, Chaos 35, 013119 (2025).
- [31] W. Deng and E. Barkai, Ergodic properties of fractional Brownian-Langevin motion, Phys. Rev. E **79**, 011112 (2009).
- [32] Y. He, S. Burov, R. Metzler, and E. Barkai, Random time-scale invariant diffusion and transport coefficients, Phys. Rev. Lett. **101**, 058101 (2008).
- [33] F. Thiel and I. M. Sokolov, Weak ergodicity breaking in an anomalous diffusion process of mixed origins, Phys. Rev. E 89, 012136 (2014).
- [34] Y. Meroz and I. M. Sokolov, A toolbox for determining subdiffusive mechanisms, Phys. Rep. 573, 1 (2015).
- [35] S. Burov, R. Metzler, and E. Barkai, Aging and nonergodicity beyond the Khinchin theorem, Proc. Natl. Acad. Sci. 107, 13228 (2010).
- [36] M. Abramovitz and I. A. Stegun, Handbook of Mathematical Functions With Formulas, Graphs and Mathematical Tables (Dover, New York, 1964).
- [37] V. Méndez, R. Flaquer-Galmés, and A. Pal, Occupation time statistics for non-Markovian random walks, Phys. Rev. E 111, 044119 (2025).
- [38] P. Lévy, Sur certains processus stochastiques homogènes, Compos. Math. 7, 283 (1940).

- [39] J. Lamperti, An occupation time theorem for a class of stochastic processes, Trans. Amer. Math. Soc. 88, 380 (1958).
- [40] W. Feller, An Introduction to Probability Theory and its Applications, Vol. II., 2nd ed. (John Wiley & Sons Inc., New York, 1971), pp. xxiv+669.
- [41] R. Gorenflo, A. A. Kilbas, F. Mainardi, and S. Rogosin, *Mittag-Leffler Function, Related Topics and Applications* (Springer, Berlin, 2020).
- [42] T. J. Kozubowski, Fractional moment estimation of Linnik and Mittag-Leffler parameters, Math. Comput. Model. 34, 1023 (2001).
- [43] K. A. Penson and K. Górska, Exact and explicit probability densities for one-sided Lévy stable distributions, Phys. Rev. Lett. 105, 210604 (2010).
- [44] R. Weron, On the chambers-mallows-stuck method for simulating skewed stable random variables, Stat. Probab. Lett. 28, 165 (1996).
- [45] M. Guéneau, S. N. Majumdar, and G. Schehr, Optimal mean first-passage time of a run-and-tumble particle in a class of onedimensional confining potentials, Europhys. Lett. 145, 61002 (2024).
- [46] E. Barkai, Residence time statistics for normal and fractional diffusion in a force field, J. Stat. Phys. 123, 883 (2006).
- [47] P. Singh, Extreme value statistics and arcsine laws for heterogeneous diffusion processes, Phys. Rev. E **105**, 024113 (2022).